Research Article

Accumulation of Microsatellite Instability in Superoxide Dismutase-1 Knockout Mice: A Possible Predictor of Germ Cell Development or Tumorigenesis

Harold Moreno-Ortiz[1,2], Clara Esteban-Pérez[1,2*], Elkin Lucena[3], Nancy A Reichert[1] and Dwayne A Wise[1]

[1]Department of Biological Sciences, Mississippi State University, Mississippi State, MS-39762, USA
[2]Colombian Center of Fertility and Sterility, CECOLFES, Bogotá, Colombia
[3]Reproductive Biomedicine, Colombian Center of Fertility and Sterility, CECOLFES, Bogotá, Colombia

Abstract

The superoxide dismutase 1 gene (*Sod1*) is one of the cell protective mechanisms to eliminate reactive oxygen species damage in order to protect cell components and avoid germinal failure or tumorigenesis. Mouse primordial germinal cells are a population of cells originating from the proximal margin of the epiblast in close proximity to the extra embryonic ectoderm, and from which some cells differentiate into male or female germinal cells. During cell migration across the genital ridge, primordial germinal cells display an extensive proliferation rate and they are exposed to ROS damage. In absence of cell antioxidant mechanisms, primordial germinal cells have increased risk to accumulate specific mutations by free radical damage. We hypothesize that during cell migration, *Sod1* knockout primordial germinal cells accumulate microsatellite instability and this could be a signal for primordial germinal cells pool selection, premature ovarian failure or tumor transformation. We dissected and isolated primordial germinal cellsfrom *Sod1*^{+/+} (wild type), *Sod1*^{+/-} (heterozygous), and *Sod1*^{-/-} (homozygous) mouse strain (B6; 129S7-*Sod1*[tm1Leb/J]), from the genital ridge at 10. 5 and 18 days post coitum to determine and quantify microsatellite instability in 10 single tandem repeat markers by single cell PCR methods. Our results demonstrate that primordial germinal cells from *Sod1*knockout mice accumulated microsatellite instability in five markers (*4-4-19844, D13mit16, D13mit78, D19mit68,* and *DXmit249*) located near important genes involved in cell proliferation and differentiation. Taken together, this study shows that microsatellite instability is directly related to *Sod1* gene disruption that could induce abnormal migration characteristics seen in primordial germinal cells such as germinal premature failure or tumor invasion and metastasis. In conclusion, microsatellite instability could be a signal for primordial germinal cells pool selection, or tumorigenesis.

Introduction

Primordial germinal cells (PGCs) are the progenitors of spermatogonia and oogonia in the testis and ovary, respectively [1]. PGCs originate from the embryonic primary ectoderm (epiblast), and they are one of the cell types that migrate directly through the developing embryo to their site of histogenesis [2,3]. Proliferation and migration of PGCs have been widely studied in different animal models such as mouse, rabbit, sheep, and pig [4]. Of all mammals studied so far, the mouse has provided the most extensive data for the study of early stages of embryonic development [5,6]. There is a similarity in development between mouse and human germinal cells. Therefore, the mouse is an outstanding research model for the study of germ cell lineage [7,8]. Our study utilizes mouse PGCs as a model to evaluate the effects of oxidative stress in germ cell development that leads to genomic instability by accumulation of microsatellite instability (MSI). Elevated free radical damage through reactive oxygen species (ROS) accumulation can override DNA repair mechanisms, giving rise to increased cell mutations that induce infertility, cancer development, chronic diseases (including cardiovascular and neurodegenerative diseases), and aging [9,10].

In mammalian cells, protection against oxidative DNA damage caused by ROS accumulation is accomplished by a complex defense system composed of antioxidant enzymes such as the superoxide dismutase family (*Sod1, Sod2,* and *Sod3*) [11]. *Sod1* is also known as copper/zinc superoxide dismutase (Cu/Zn Sod). *Sod2* is also known as manganese superoxide dismutase (Mn-Sod), and *Sod3* is also known as secreted extracellular superoxide dismutase (EC-Sod). All of these *Sod* genes play critical roles in order to maintain cell oxidative homeostasis

and are expressed in the rodent ovary and testis [12]. The *Sod1* gene codes for cytosolic superoxide dismutase, which is important for the catalyzation of superoxide ion (O_2^-) into hydrogen peroxide (H_2O_2), and in presence of catalase, H_2O_2 is reduced to water [13]. The *SOD1* enzyme has been isolated from a wide range of organisms such as yeast, bacteria, mice, chicken, and bovine [14]. *Sod1* mutant mice display a pleiotropic phenotype that includes neurodegeneration, immunodeficiency, cancer predisposition, and hypersensitivity to ionizing radiation [15]. Although *Sod1* knockout mice are born and develop normally, *Sod1* deficient female mice are sub-fertile or infertile and display a marked increase in post-implantation embryonic lethality [16]. Altogether, *Sod1* deficient mice are prone to infertility and cancer due to an increase of ROS within the ovary affecting its function. Recent observations related to fertility and *Sod1* knockout mice are correspondent. Watanabe et al. [17] concludes that *Sod1* knockout female mice show repression of plasma progesterone level compared to *Sod1*^{+/+} females during pregnancy. Also, *Sod1* knockout oocytes could be normally fertilized and developed to the two-cell stage *in vitro*. However, *Sod1* knockout

embryos failed to divide to the four-cell stage under conventional culture conditions (20% O_2). When *Sod1* knockout embryos were cultured under hypoxic conditions (1% O_2), they developed to the morula stage but could not develop into blastocysts, indicating that O_2 stress inhibited the development of *Sod1* knockout embryos at the two-cell stage. Also, Noda et al. [18] concludes that fertilization of the oocytes *in vitro* conditions was normal, however the development of the embryo was impaired by the deficiency of lutea support that ensure the progress of implantation and pregnancy [17]. This increased ROS to which the *Sod1* knockout mice are exposed, results in inhibition of downstream genetic mechanisms that are responsible for the increased risk of ovarian follicular dysfunction and are at a higher risk for premature ovarian failure and cancer development [19].

Endogenous production of ROS from different cellular metabolic processes leads to persistent exposure to oxidative damage [14]. Protective mechanisms against this damage are needed in order to counteract harmful effects in vulnerable cell components such as mitochondria, nucleus, and membrane [9]. However, mutations in the genes responsible for removing superoxide radicals generated in the cytoplasm and nucleus can have a negative impact on genomic DNA integrity, giving rise to defects in cell functionality and cell malignancy transformation [14]. In order to analyze the role of the *Sod1* gene in genomic homeostasis of mouse PGC development, we dissected and isolated primordial germinal cells from the genital ridges of *Sod1* $^{+/+}$ (wild type), *Sod1* $^{+/-}$ (heterozygous), and *Sod1* $^{-/-}$ (homozygous) mice. Our results support the hypothesis that accumulation of genomic DNA instability due to oxidative damage, established by MSI, is a main factor that negatively influences cell development and cell migration. MSI was detected in different mouse single tandem repeats in *Sod1* homozygous -/- mouse embryos at 10. 5 days post-coitum (dpc). This study suggest that these markers are important novel target sequences that could be used in humans as a screening method to evaluate the disruption of cell stress responses that lead to initiation and progression of premature ovarian failure or ovarian carcinoma.

Materials and Methods

Animal model

Uteri of pregnant female mice from the heterozygous superoxide dismutase 1 (*Sod1*) knockout strain (B6; 129S7-*Sod1*$^{tm1Leb/J}$) were purchased from The Jackson Laboratory (Bar Harbor, ME). Details related to the generation of the *Sod1* mouse model have been previously described. Briefly, target mutations in the *Sod 1* gene were generated by replacement of exon 1 and 2 with a PGK-hptr expression cassette [12]. In the Jackson Lab facilities, male and female heterozygous mice with the superoxide dismutase 1 (*Sod1*^{tm1Leb}) gene were bred. Females were checked for vaginal plugs and plug-positive females were transferred to necropsy at 10. 5 and 18 days post-coitum (dpc). Uteri were removed from euthanized females and shipped to our laboratory at Mississippi State University. A total of two pregnant uteri at 10. 5 dpc and two uteri at 18 dpc were dissected. From these uteri we obtained a total of 37 mouse fetuses: male (n=18) and female (n=19, with the three expected genotypes: wild type homozygous *Sod1*$^{+/+}$(n=11), heterozygous *Sod1*$^{+/-}$ (n= 20), and homozygous *Sod1*$^{-/-}$(n=6).

Isolation and maintenance of primordial germinal cells

From each mouse fetus, the placenta and extra embryonic tissues were removed. Mouse fetuses were transferred into a fresh petri dish filled with D-PBS and the length was measured. Fetus tails were removed for DNA purification, sexing, and genotyping by PCR. Each mouse fetus was dissected following the protocol previously standardized in our lab [20]. Briefly, gonadal ridges were removed by cutting away the tissues that support them. Gonadal ridges were transferred to a petri dish filled with fresh PBS to clean away the surrounding somatic cells. Dispersed suspensions of PGCs from the containing tissues were recovered for isolation of DNA. Characterization of PGCs was achieved using the alkaline phosphatase kit according to the manufacturer's instructions (Millipore, Billerica, MA).

DNA isolation

DNA was prepared from each fetus tail and from primordial germinal cells harvested from gonadal ridges at 10. 5 and 18 dpc. DNA was isolated with the Purelink genomic DNA mini kit (Invitrogen Carlsbad, CA) following the manufacturer's protocol. All DNA samples were quantified using a NanoDrop™ ND1000 spectrophotometer (Thermo Scientific, Wilmington, DE).

Sex determination of mouse fetus

Sex determination was achieved by PCR amplifications performed in a total reaction volume of 25μl containing 1X of buffer D (US DNA, Forth Worth, TX), 2. 5mM ofMgCl (US DNA, Forth Worth, TX), 10mM of dNTPs (Applied Biosystems, Foster City, CA) and 1. 25 U/μL of hot multi taq DNA polymerase (5 U/μl; US DNA, Forth Worth, TX). Primers were used as follows: Zfy forward 5'-AAGATAAGCTTACATAATCACATGGA and Zfy reverse 3'-CCTATGAAATCCTTTGCTGCA CATGT, 600bp. The m-DXNds3 forward: GAGTGCCTCATCTATACTTACAG and m-DXNds3 reverse: TCTAGTTCATTGTTGATTAGTTGC, 242 bp [21]. PCR was performed on PE 9600 thermocycler using following cycling protocol: 1 cycle of 95°C for 11 min, 30 cycles of (denaturation for 60 sec at 94°C, annealing for 150 sec at 60°C, and extension for 150 sec at 72°C) final step 1 cycle of 72°C for 2 min and hold at 4°C. Negative controls were included in each PCR. Amplified products were analyzed with gel electrophoresis at 4% nusieve agarose gel (Clonetics, Lonza, Walkersville, MD).

Genotyping of mouse fetus

Genotyping of mouse fetuses to determine presence of the *Sod1* transgene was achieved by PCR amplifications performed in a total reaction volume of 25 μl containing 1X of buffer D (US DNA, Forth Worth, TX), 2. 5mM of MgCl (US DNA, Forth Worth, TX), 10 mM of dNTPs (Applied Biosystems, Foster City, CA) and 1. 25 U/μL of hot multi taq DNA polymerase (5 U/μl; US DNA, Forth Worth, TX). Primers used were: Mut781F 5'-TGTTCTCCTCTTCCTCAT CTCC-3', Mut782R 5'-ACCCTTTCCAAATCCTCAGC-3', Wt878F 5'TGAACCAGTTGT GTTGTCAGG-3', and Wt888R 5'-TCCATCACTGGTACAT AGCC-3' (The Jackson Lab, Bar Harbor, ME). PCR reactions were performed on PE 9600 thermocycler using cycle as follows: 1 cycle for 94°C for 3 min, 35 cycles of (94°C for 20 sec, 60°C for 1 min; 72°C for 1 min); 1 cycle 72°C for 2 min, and hold at 4°C. Negative controls were included in each PCR. Amplified products were analyzed with gel electrophoresis at 4% nusieve agarose gel (Clonetics-Lonza, Walkersville, MD).

Mouse single tandem repeat markers selection and standardization

A total of 21 single tandem repeats (STR) were selected from across the mouse genome. Fifteen markers were located on autosomes, and six markers were located on X chromosome (Table 1). Fluorescent primers were purchased from IDT (Coralville, IA) at 100μM/μL. The labeled dyes used were either 6-FAM (blue) or HEX (green). For initial testing, forward and reverse primers were combined for a final primer concentration of 25μM/μL to create a singleplex primer stock. Primers

were tested at concentrations ranging from 0. 8-1. 5 μM/μL in standard PCR conditions and reagents. Each locus was standardized in separate PCR reactions for optimization and to ensure specificity and sensitivity of the marker.

Single cell PCR

PCR was performed for 10 markers out of 21 total markers because only these 10 markers amplified during standardization. Two markers came from the mouse X chromosome, one marker each from

chromosomes 6 and 17, and two markers each from chromosomes 8, 13, and 19 (Table 2). DNA serial dilutions were made at 0. 1 ng/μL, 0. 05 ng/μL, and 0. 025 ng/μL. Using these serial DNA dilutions, Poisson analysis of the amplified alleles was performed to calculate the correct genomic equivalent value for each sample in order to obtain less than one diploid genome equivalent of the DNA sample (sample genome equivalents range between 12. 5-50 pg/μL) [22,23]. This concentration of DNA allowed sufficient sensitivity to distinguish between wild type and mutated alleles at their appropriate frequency.

PCR amplifications were performed in a total reaction volume of 10 μl containing 1 X of buffer D [800 Mm Tris HCl, 200 mM $(NH_4)_2SO_4$, 0. 2% w/v Tween 20](US DNA,Fort Worth, TX), 2. 5 mM $MgCl_2$ (US DNA, Fort Worth, TX), 1 X of Solution L(US DNA,Fort Worth, TX),1. 25 U Hot-MultiTaq DNA polymerase (5 U/μl; US DNA,Fort Worth, TX), 4% DMSO (Sigma Aldrich, Saint Louis, MO), 0. 4 mg/μLbovine albumin serum (Thermo Scientific, Rockford, IL), 300μM dNTPs (Applied Biosystems, Foster City, CA), and 0. 5 and 1. 8 μM mixed primer (forward and reverse) respectively. Solution L (1X) was used as an additive that facilitates amplification of difficult templates. PCR was performed on a PE 9600 thermocycler using a ramping cycling protocol: 1 cycle of 95 ºC for 11 minutes; 1 cycle of 96 ºC for 1 minute; 10 cycles of [94ºC for 30 seconds, ramp 68 seconds to 58 ºC (hold for 30 seconds), ramp 50 seconds to 70 ºC (hold for 60 seconds)]; 25 cycles of[90 ºC for 30 seconds, ramp 60 seconds to 58 ºC (hold for 30 seconds), ramp 50 seconds to 70 ºC (hold for 60 seconds)]; 1 cycle of 60ºC for 30 minutes for final extension; and hold at 4ºC. Negative controls and reaction mixtures were included in each PCR to monitor for contamination.

Products amplified by single genome equivalent PCR were separated and detected by fragment analysis on an AB 3130XL Genetic Analyzer (Applied Biosystems, Foster City, CA) in the presence of Gene Scan 500 LIZ Ladder (Applied Biosystems, Foster City, CA) following the manufacturer's protocol. Wild type and mutated alleles were quantified with the Gene Mapper version 4. 0 software package (Applied Biosystems, Foster City, CA). Repeat motif shifts from wild

N.	Marker	Size (Bp)	Repeat Motif	Marker Location
2	M4-4	137	(CTTTT)17	Chrom 4
3	M4-2	129	(GAAAAA)9	Chrom 4
4	mBat37	121	(A)37	Chrom 6
5	D8mit120	130	(GT)28	Chrom 8
6	D8mit47	198	(TG)14	Chrom 8
7	D8mit88	113	(TG)14	Chrom 8
8	D13mit16	209	(TG)24	Chrom 13
9	4-4-13-45870	390	(GAGAA)40	Chrom 13
10	D13mit78	225	(CA)25	Chrom 13
11	D14mit5	178	(GT)9	Chrom 14
12	MT2620	99	(CA)13	Chrom 15
13	D17mit20	176	(CATA)13	Chrom 17
14	4-4-19844	280	(CAGGCT)30	Chrom 19
15	D19mit68	132	(TG)21	Chrom 19
16	DXmit54	192	(CA)15 (GA)16	Chrom X
17	DXmit249	114	(TG)17	Chrom X
18	DXmit116	102	(CA)19	Chrom X
19	DXmit192	123	(CA)24	Chrom X
20	mBat-24	98	A(24)	Chrom X
21	MX-3	115-121	(CA)19	Chrom X

Notes: Fifteen markers were located in various autosomes. Six markers were located in the X chromosome. This table depicts the size in base pairs (bp), repeat motifs, and the chromosome location

Table 1: Complete list of 21 microsatellite mouse markers.

n.	MARKER	CHROMOSOMAL LOCATION (cM)	SIZE (bp)	REPEAT MOTIF	GENBANK NUMBER	PRIMER SEQUENCES	FLUORESCENT LABELS
1	mBat24	ChrXq26.1	98	(A)24	14734	CATAGACCCAGTGCTCATCTTCGT CATCGGTGGAAAGCTCTGA	HEX
2	D13mit78	Chr13 (75.0)	225	(CA)25	62142	ACAGCACGGGTTTATCATCC TATGCCTGCCAGGCTTCTAT	HEX
3	DXmit249	ChrX(60.5)	114	(TG)17	493105	TTATGTGCTTATTAGCCAAGGTG AAAATAGAACTTCAGCAGCATGC	HEX
4	D19mit68	Chr19 (6.0)	132	(TG)21	16973	CCAATACAAATCAGACTCAATAGTCG AGGGTCTCCCCATCTTCCTA	HEX
5	D8mit47	Chr8 (56.0)	197	(TG)14	109384	AAGATGTGCTTACTCTGACTTCCC GGATCTATCCACATGTGGTGC	HEX
6	D8mit88	Chr8 (61.66)	113	(CA)14	94457	GTCCCTTGTAAACACTCTTGCC CTCTTTGCCCACGGTTATGT	HEX
7	D17mit20	Chr17 (34.3)	176	(CATA)13	12266	AGAACAGGACACCGGACATC TCATAAGTAGGCACACCAATGC	HEX
8	D13mit16	Chr13 I (10.0)	207	(TG)24	109406	CCAGCTGAAGGCTTACTCGT AAAGTTAGAATCAGCCATTCAAGG	FAM
9	mBat37	Chr6qC3 (35.94)	121	(A)37	1350935	TCTGCCCAAACGTGCTTAAT CCTGCCTGGGCTAAAATAGA	FAM
10	4-4-19-844	Chr19 (42.0)	280	(CAGGCT)30	R96357	CAGTTCACAGGGTAGCCACA AAGGTACTGCACCTGCTTGG	FAM

Notes: This table shows the specific chromosome location, size of marker (bp), repeat motifs, genbank access number, primer sequences amplified and dye labels for each marker

Table 2: Microsatellite markers for detection of MSI in primordial germinal cells of mouse.

type standardized alleles were considered mutant alleles [22,23]. Presence of wild type and/or mutant alleles was scored for each single cell replicate. An average of 48 replicates per sample were amplified and scored from different samples of mouse PGCs.

Genomic instability statistical analysis

We amplified less than a single diploid genome-equivalent of DNA with single cell PCR methods to estimate oxidative stress-induced mutation frequencies in specific microsatellite repeat markers. DNA concentrations were adjusted to obtain between 0. 5-2 genome equivalents, on average, per single cell PCR reaction. The average number of amplifiable DNA molecules (λ) in each PCR reaction was calculated using the Poisson distribution: $\lambda = -\ln(K_l/K)$, where $K_l =$ the total number of alleles expected minus the number of alleles observed, and K =the total number of alleles expected [22,24,25].

Mutation frequencies for each marker by sample genotype, sex, and age were calculated by SP-PCR software version 2. 0 (M. D. Anderson Cancer Center, Houston, TX). Maximum likelihood estimates of the mean number of mutant alleles and wild type alleles in each replicate, as well as their bootstrap standard deviations, were also calculated by SP-PCR software version 2. 0 (M. D. Anderson Cancer Center, Houston, TX). Differences in the estimation of mutation frequencies were calculated with a two tailed t-test using raw mutation frequencies. A three way cross class ANOVA, assuming no third factor interaction, and appropriate LSD multiple comparison (t-test) outputs were also produced. Results were considered statistically significant with a $p<0.05$ (using Procedure GLM from statistical package SAS/win 9. 2, SAS Institute Inc. , Cary, NC).

Results

Sod1$^{-/-}$ knockout genotype could be responsible for embryo growth retardation or loss of pregnancy

We obtained two mouse uteri from The Jackson Laboratory at 10. 5 dpc and two uteri at 18dpc. Fetal genotypes were determined with PCR using purified DNA samples of mouse fetus tails dissected during the isolation protocol. We were able to genotype the following 37 fetuses: 19 females including 8 $Sod1^{+/+}$, 9 $Sod1^{+/-}$, and 2 $Sod1^{-/-}$, and 18 male fetuses including 3 $Sod1^{+/+}$, 11 $Sod^{+/-}$, and 4 $Sod1^{-/-}$ (Figures
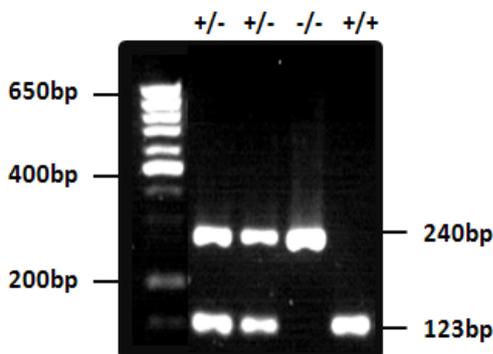

Figure 1: Determining genotype of mouse fetuses with STS markers: *MR0781* and *MR0878*

Notes: Amplifications from STS markers: *MR0781* and *MR0878* were analyzed through gel electrophoresis a 4% NuSieveagarose gel.1000bp ladder (EZ BioResearch LLC, Saint Louis, MO) (line1). *Sod1* heterozygous (+/-) samples showed both 240 bp and123 bp bands (lines 2 and 3). *Sod1* homozygous (-/-) samples showed only 240 bp band (line 4). *Sod1* homozygous (-/-) wild type samples showed only 123 bp band (line 5).
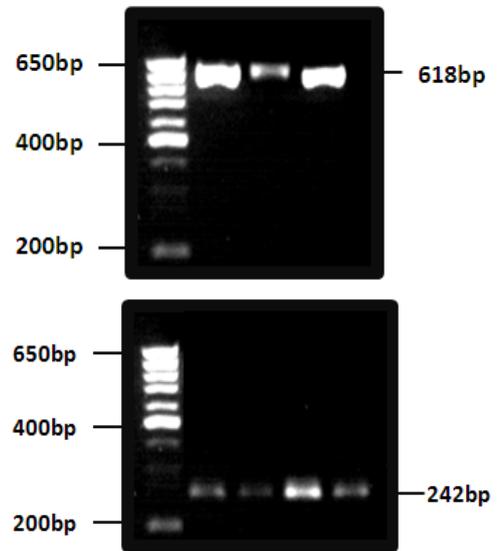

Figure 2: Determining sex of mouse embryos with sex specific STS markers: *Zfy* and *DXNd3fR*

Notes:Amplifications from STS markers: *Zfy*and *DXNd3fR* were analyzed through gel electrophoresis in a 4% NuSieveagarose gel. *Zfy* (618 bp) will only amplify for males and *DXNd3fR* (242 bp) will amplify for the presence of X chromosome. A) 1000 bp ladder (EZ BioResearch, LLC, Saint Louis, MO) (line1).*Zfy*amplification (618bp) band from three male mouse embryo samples (lines 2-4).B) 1000 bp ladder (EZ BioResearch, LLC, Saint Louis, MO) (line1). *DXNd3fR* amplification (242 bp) band in four mouse female embryos.
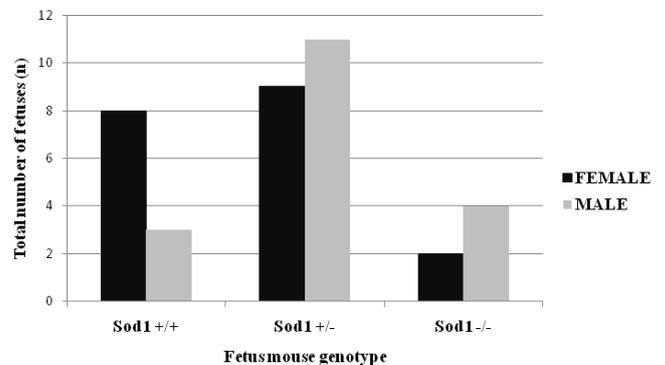

Figure 3: Total number of fetuses dissected from mouse uteri according to genotypes.

1-3). Drastic reduction in the physical size of female homozygous $Sod1^{-/-}$ mouse fetuses was observed. These results suggest that the reduced number of the female $Sod1^{-/-}$ phenotype might be the result of sub-fertility due to early embryonic reabsorption or spontaneous miscarriage (Figure 3). However, this observation was not statistically significant. The lengths of all dissected fetuses were measured, and we observed that at 10. 5 dpc of gestational age, male and female $Sod1^{+/+}$ (wild type) and heterozygous $Sod1^{+/-}$ mouse fetuses showed an average size of 14mm. In contrast, female homozygous $Sod1^{-/-}$ mouse fetuses showed a slight decrease in average size at 10 mm, and male homozygous $Sod1$-/- mouse fetuses showed an average size of 13 mm. At 18dpc, all fetuses showed an average size of 21 mm for all genotypes, and no differences between male and female fetuses were observed (Figure 4).

Genomic instability in single tandem repeats was present in *Sod1* knockout mice

Cancer and other disorders such as infertility have been correlated with accumulation of spontaneous mutations due to oxidative stress in different organs such as brain, testes, ovary, and liver [26]. Mechanism of cellular defense against oxidative stress includes *Sod1* which is a key
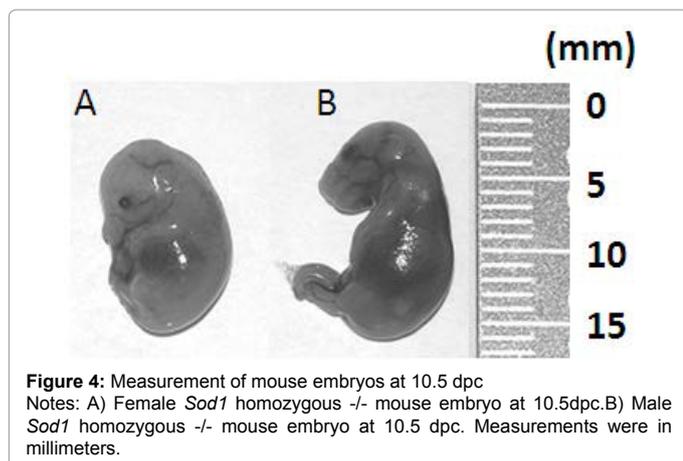

Figure 4: Measurement of mouse embryos at 10.5 dpc
Notes: A) Female *Sod1* homozygous -/- mouse embryo at 10.5dpc.B) Male *Sod1* homozygous -/- mouse embryo at 10.5 dpc. Measurements were in millimeters.
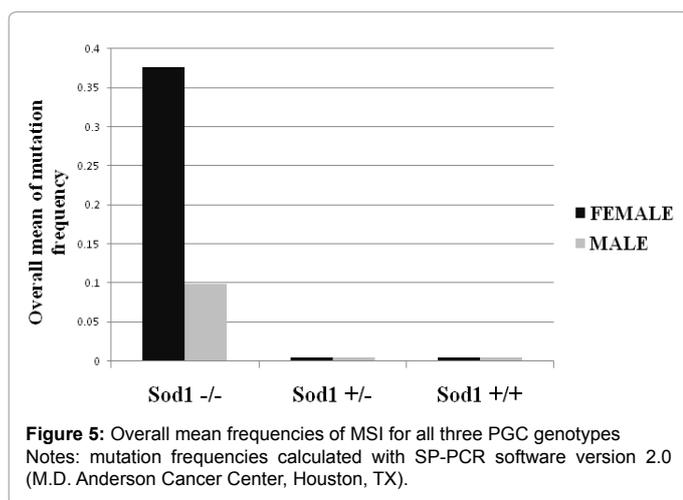

Figure 5: Overall mean frequencies of MSI for all three PGC genotypes
Notes: mutation frequencies calculated with SP-PCR software version 2.0 (M.D. Anderson Cancer Center, Houston, TX).

molecule in the redox system [14]. We asked whether disruption of the *Sod1* function induces accumulation of the spontaneous mutations in PGCs early in embryonic development at 10. 5 dpc and later on at 18 dpc. We determined genomic instability by MSI analysis at two different times during mouse embryonic germinal cell development (10. 5 dpc and 18 dpc). DNA samples from female and male PGCs of *Sod1*^{+/+}, *Sod1*^{+/-}, and *Sod1*^{-/-} genotypes were analyzed. We observed statistically significant high frequencies of mutations in five out of 10 microsatellites evaluated (*4-4-19844*, *D13mit16*, *D13mit78*, *D19mit68*, and *DXmit249*) (Figure 5) (Table 3). These results show that spontaneous mutations can accumulate in microsatellite sequences during embryonic development due to a deficiency in mouse PGCs to oxidative stress response.

Microsatellite instability occurs early in the mouse PGC development

Mouse PGCs migrate out of the hindgut through the dorsal mesentery at 9. 5 dpc. PGCs arrive at the genital ridge at 10. 5-11. 5 dpc. The complete colonization of the genital ridge by PGCs is achieved at 13 dpc. After PGC migration and colonization, the percentage of PGCs gradually decline from 13. 5 dpc to 16. 5 dpc of mouse embryonic development [27]. We suggest that accumulation of MSI could be the signal on the genital ridge for PGC selection before meiotic arrest takes place. Our results report high mean frequencies of MSI in *Sod1* knockout mouse PGC samples, whereas wild type *Sod1* and heterozygous *Sod1*^{+/-} mouse PGC samples did not show MSI over time. Specifically female PGCs *Sod1* knockout -/- at 10. 5 dpc showed a high overall mean frequency of MSI in four unstable markers (f= 0. 362) in comparison with the MSI frequency observed just in one unstable marker at 18 dpc (f= 0. 012). Our results suggest that MSI could be a signal for PGC pool selection during early mouse gonad colonization in embryos with abnormal redox mechanisms (Table 3).

Oxidative stress response due to superoxide dismutase 1 deficiency differs between sexes

Previous studies have reported that female *Sod1* knockout mice are infertile in comparison with male homozygous mice that are reproductively normal [12,16]. We were interested in determining if MSI accumulation is common in female or male PGCs from *Sod1* knockout mouse embryos. Our results showed high MSI frequency in female and male *Sod1* knockout mouse PGCs. Female *Sod1* knockout PGCs showed statistically high MSI frequencies in four markers at 10. 5 dpc (*4-4-19844*, *D13mit16*, *D13mit78*, and *DXmit249*) and only one

| Gender | Genotype | Embryo Age (Days post-coitum) | LOCI* | | | | | | | | | | | | | | |
| | | | *4-4-19844* | | | *D13mit16* | | | *D13mit78* | | | *DXmit249* | | | *D19mit68* | | |
			n	m	f	n	m	f	n	m	f	n	m	f	n	m	f
Male	Mutated	11 dpc	37	0	0	35	2	0.031	28	0	0	28	2	0.062	33	2	0.055
		18 dpc	45	0	0	34	0	0	28	0	0	38	0	0	44	0	0
	Heterpzygous	11 dpc	14	0	0	44	0	0	36	0	0	46	0	0	47	0	0
		18 dpc	27	0	0	44	0	0	28	0	0	40	0	0	42	0	0
	Wild type	11 dpc	41	0	0	44	0	0	41	0	0	30	0	0	41	0	0
		18 dpc	46	0	0	91	0	0	42	0	0	43	0	0	44	0	0
Female	Mutated	11 dpc	26	3	0.075	26	2	0.051	22	5	0.15	39	7	0.086	41	0	0
		18 dpc	36	0	0	42	0	0	39	1	0.012	48	0	0	48	0	0
	Heterpzygous	11 dpc	45	0	0	46	0	0	39	0	0	47	0	0	48	0	0
		18 dpc	74	0	0	82	0	0	45	0	0	42	0	0	42	0	0
	Wild type	11 dpc	40	0	0	42	0	0	35	0	0	43	0	0	41	0	0
		18 dpc	30	0	0	46	0	0	44	0	0	40	0	0	40	0	0

Notes: *Number of estimated alleles (n), number of mutant alleles (m), and mutation frequency (f) were calculated using SP-PCR software version 2.0 (M.D. Anderson Cancer Center, Houston, TX)

Table 3: Frequencies of MSI at five significantly informative microsatellite markers in male and female mouse primordial germinal cells.

marker showed instability at 18 dpc (*D13mit78*). In contrast, male *Sod1* knockout PGCs showed instability frequencies in three markers at 10. 5 dpc (*D13mit16, D19mit68,* and *DXmit249*) and no instability was detected at 18 dpc. Female *Sod1* knockout PGCs displayed a significant 3-fold increase in the overall mean mutation frequency compared with male *Sod1* knockout PGCs (p<0. 05) (Figure 6). Mutation frequencies in wild type and heterozygous *Sod1* were stable in both female and male PGCs samples. These observations confirm that MSI could be the cause of female *Sod1* reproductive deficiency.
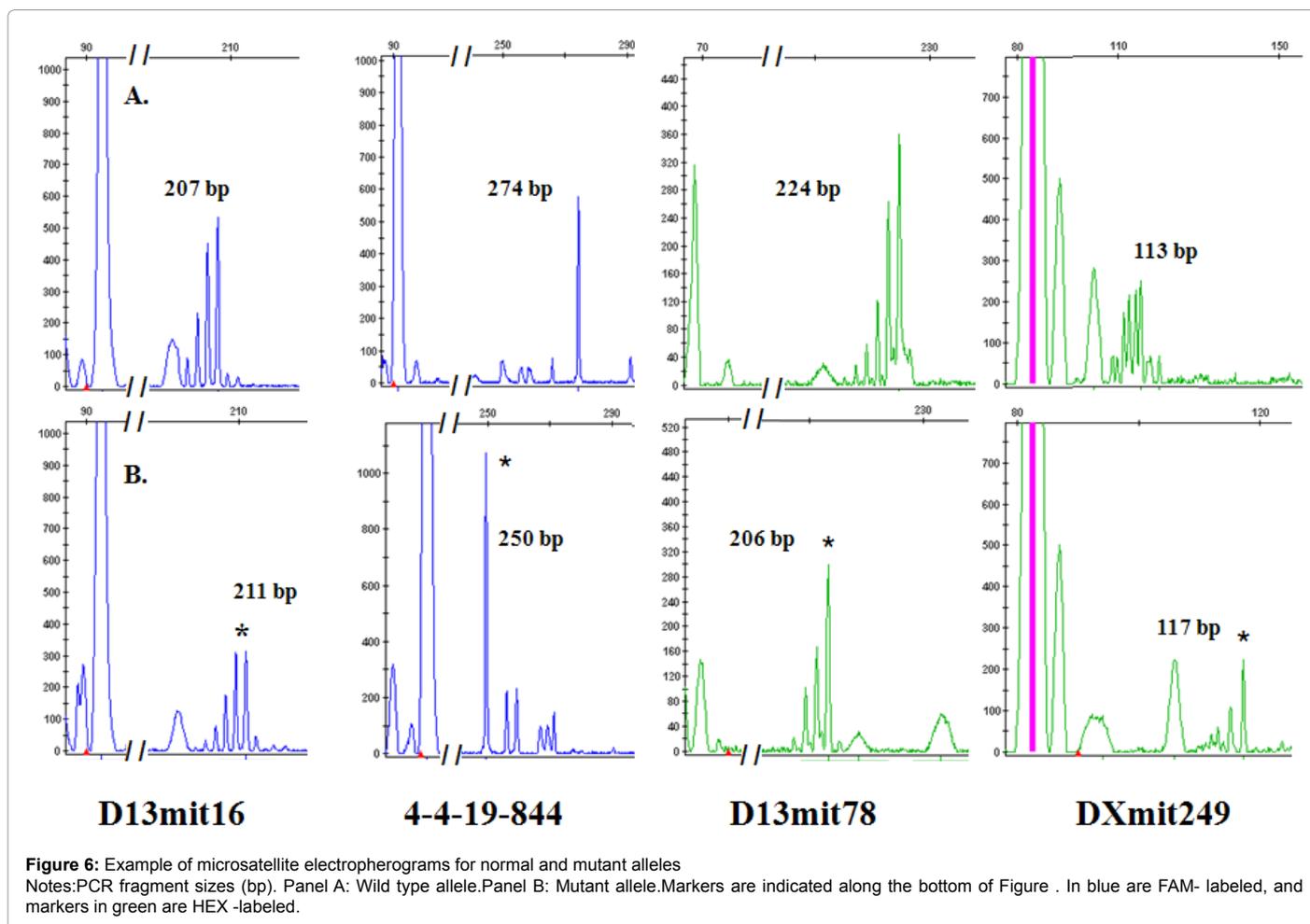
Microsatellite instability was detected in markers located near genes responsible for cellular stress responses

Upon migration and colonization of genital ridge by PGCs, several molecular pathways are responsible for the establishment of germinal cell pool during the mouse embryonic development [28]. Deregulation of *Sod1* gene is a perfect model to evaluate oxidative stress damage as a cause of disease [29,30]. We determined MSI frequencies in two markers in both female and male knockout *Sod1* mice. One marker is located near a gene involved in counteracting the oxidative damage mechanism (*Dxmit249*) and the other marker has been linked to migration and colonization status of PGCs (*D13mit16*). Significant differences in MSI frequencies were obtained with these two markers at 10. 5 dpc between female and male PGC samples. High MSI frequencies in both markers were observed in female and male *Sod1* knockout mice compared to female and male wild type and heterozygous +/- *Sod1* mice (p<0. 0001). *Dxmit249* marker was highly unstable compared to *D13mit16*

at 10. 5 dpc in female and male *Sod1* knockout mice (Figure 7). At 18 dpc both markers were stable. Our results indicate that MSI detected in markers located near genes responsible for the downstream steps in the antioxidant *Sod1* pathway could be the signal for oxidative stress damage.

Embryonic development is disrupted by the presence of MSI in genes responsible for cell lineage commitment

Early during mouse embryonic development, primordial germinal cells are derived from the embryonic primary ectoderm (epiblast) [2]. Developmental genes responsible for cell lineage commitment are targets for the accumulation of spontaneous mutations generated by deregulation of antioxidative pathways [31]. We wanted to demonstrate that MSI is present near genes involved in embryonic differentiation pathways. We found that MSI was present in two unstable markers related to key genes that play a role in the morphogenesis stages of the embryo (*D13mit78* and *4-4-19844*). Significant differences in MSI frequency were observed in female *Sod1* knockout PGCs when compared to male *Sod1* knockout PGCs, which were stable for these two markers. The MSI detected in the *D13mit78* marker was highly significant at 10. 5 dpc in the female *Sod1* knockout PGC sample (f=0. 14 p=0. 0001) compared to the MSI frequency of marker *4-4-19844* (f=0. 074 and p=0. 0002) (Figure 8). Unstable alleles were not detected in either wild type *Sod1*^{+/+} PGC or heterozygous *Sod1*^{+/-} PGC samples. Taken together, these findings demonstrate that MSI could be a signal that triggers deregulation of genes involved in germ cell lineage commitment.
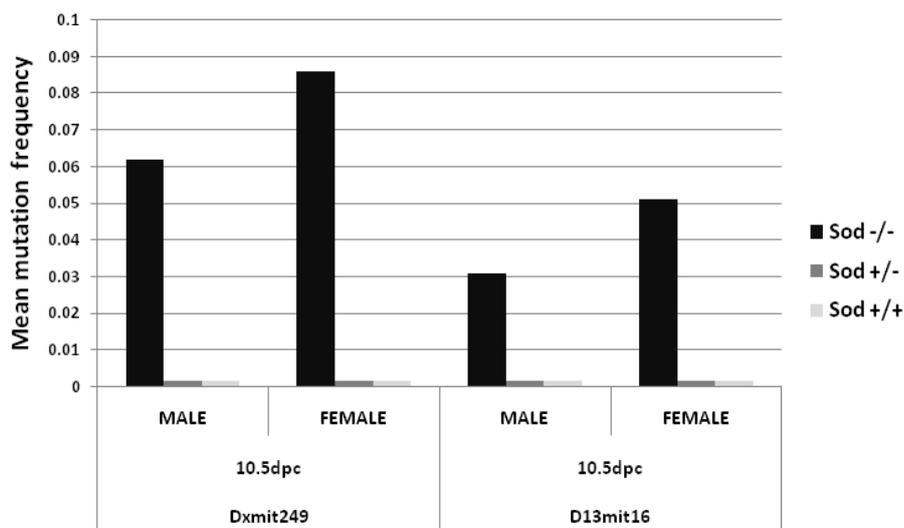

Figure 6: Example of microsatellite electropherograms for normal and mutant alleles
Notes:PCR fragment sizes (bp). Panel A: Wild type allele.Panel B: Mutant allele.Markers are indicated along the bottom of Figure . In blue are FAM- labeled, and markers in green are HEX -labeled.

Figure 7: Significantly high MSI in *Dxmit249* and *D13mit16*

Notes: MSI for these markers were detected in both male and female *Sod1 -/-* knockout PGC samples at 10.5dpc. No MSI was detected at 18dpc.
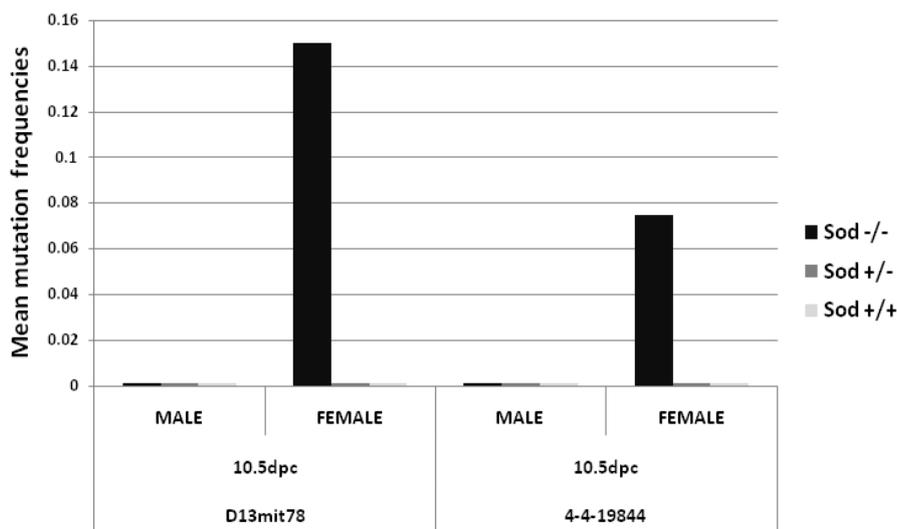

Figure 8: Significantly high MSI in *D13mit78* and *4-4-19844* markers

Notes: MSI for these markers were detected in female *Sod1 -/-* knockout PGC samples at 10.5dpc. No MSI was detected at 18dpc.

Male PGCs are sensitive to microsatellite instability in specific markers related to Wnt cofactor genes

The Wnt signaling pathway participates in embryogenesis. This pathway controls cell proliferation and migration of mouse PGC and is thought to be related to specific functions in gonad and germ cell development [32]. We detected MSI in one marker (*D19mit68*) that is associated with Wnt cofactor responsible for the intracellular signaling cascade in mouse embryonic development. However, only male *Sod1* knockout PGCs were unstable for this marker, and significant MSI frequency was observed in *D19mit68* at 10. 5 dpc (p=0. 0067) (Figure 9). This marker was stable in both *Sod1* wild type and *Sod1* heterozygous male and female mice of all genotypes. Some non-significant instability was detected in PGCs at 18 dpc in both *Sod1* wild type and *Sod1* heterozygous male and female mice of all genotypes. This result is congruent with the importance of the Wnt signaling cascade function reported by others [33]. MSI detection in this marker could be a signal to deregulate the initializing cofactor for this important developmental pathway due to accumulation of mutations in mouse PGCs.

Discussion

Characterization of embryonic germinal cells as precursors to male or female gonads in mammals is essential for designing research related to infertility, gametogenesis, and cancer during early development. The numerous possible uses of these cell lines for further basic studies made them an invaluable research tool. Investigations of oxidative stress as a cellular mechanism involved in accumulation of mutations in tumorigenesis, disease development, or cell aging have increased our understanding about different pathways of cell pathogenesis. It is
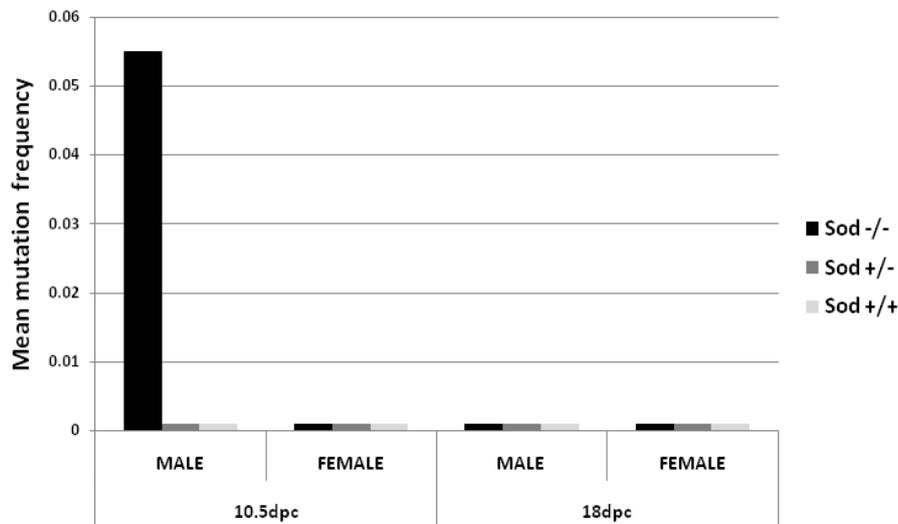
Figure 9: Significantly high MSI in D19mit68 marker

Notes: MSI was detected for *D19mit68* marker in male *Sod1* -/- knockout PGC samples at 10.5dpc. No MSI was detected at 18dpc.

well understood that cells increase the rate of MSI due to accumulation of DNA damage that override DNA repair mechanisms and tumor suppressor pathways, leading to a best-case scenario of apoptosis or a worst-case scenario of tumor transformation. Many mouse models have been developed to study cellular stress response signals [12]. Knockout mice for the *Sod1* gene, an antioxidant molecule responsible for the cellular stress response that defends against damage accumulation from oxidative stress, is a notable research model used in our study. Associated with the aging process, *Sod1* knockout mice have displayed increases in DNA damage and MSI that are involved in the induction of spontaneous tumors such as in lymphoma, liver, and spleen cancer [12,26,34]. Additionally, these knockout *Sod1* mice have developed neurodegenerative disorders such as amyotrophic lateral sclerosis and Parkinson's disease that have been linked to the oxidative damage [35].

This mouse knockout strain (B6; 129S7-*Sod1*^tm1Leb/J) is an ideal model for our study on the etiology of early ovarian cancer signals. This model has led us to understand and clarify early molecular signals implicated during ovarian development, ovarian tumor transformation, and ovarian cancer progression due to the accumulation of DNA damage by oxidative stress. Genomic instability in PGCs might be the first step of impairment for cell migration and early differentiation in the genital ridges. Our focus is the study of possible signals of genomic instability that induce germinal mutations during the first germ cell commitment in embryonic development. It is known that these signals have been linked to the origin of different cancers such as breast and endometrial carcinomas.

Our results indicate that PGCs accumulate MSI in particular markers located near important genes involved in cell proliferation, differentiation, and migration. This event could be a signal that modulates gonadal colonization by PGCs and selection of the germ cell pool that will be arrested for future gametogenesis in adult mice. We found that PGCs on *Sod1* knockout mice have increased spontaneous mutations as determined by detection of high frequencies of MSI in five out of ten markers we tested. Female and male *Sod1* knockout mice were significantly unstable in contrast to the complete stability detected for PGCs samples from *Sod1* wild type and *Sod1*^+/- heterozygous mice.

The induction of MSI in mouse PGC samples from female and

male *Sod1* knockout embryonic mice are directly related to the increased sensitivity of spontaneous mutations due to antioxidant defense disruption. Furthermore, our results were in agreement with the observation that *Sod1* knockout females are reproductively deficient while *Sod1* knockout males are fertile [12]. PGC samples from female *Sod1* knockout mice showed instability in four markers located near genes previously linked to neuroectoderm cell lineage commitment and ovarian cancer development. These genes are responsible for normal migration and colonization abilities of the embryonic germinal tissue early during development as well in abnormal invasion and metastasis abilities seen during cell transformation and tumorigenesis.

Female and male *Sod1* knockout PGCs were significantly unstable for markers *Dxmit249* and *D13mit16* in contrast with female and male *Sod1* wild type and *Sod1*^+/- heterozygous mice who were stable. Marker *Dxmit249* is near the carbonic anhydrase 5b, mitochondrial (*Car5b*) gene that is involved in the conversion of pyruvate to lactic acid in the presence of oxygen. The *Car5b* gene catalyzes the reversible hydratation of CO_2 to HCO_3 in order to maintain tissue pH homeostasis [36]. In cancer cells, high levels of intracellular lactate give rise to over expression of acid-regulating proteins like carbonic anhydrases [37] (Table 4). Our results infer that MSI of marker *Dxmit249* could be a signal that deteriorates pH cell defense mechanisms implicated in ovarian cancer disease. Marker *D13mit16* is located near engulfment and cell motility protein 1(*Elmo1*) gene that is responsible for stimulation of normal cell migration. Although its role in different cell processes has not been clearly defined, it is known that *Elmo1* protein links to *Dock180* protein to form a protein complex (*Dock180-Elmo1* complex) that plays a critical role in cell adhesion, proliferation, dissemination and invasion of ovarian cancer [38] (Table 4). The *Dock180-Elmo1* complex activates *Rac1*, a member of the Rho GTPase family, which participates in the modulation and regulation of the actin cytoskeleton that is essential in cell migration during cancer cell invasion [39]. Our results suggest that MSI in marker *D13mit16* could be an early manifestation of the invasive potential that ovarian cancer cells display at the adult stage. However, further studies are needed to conclusively determine the role, if any, that MSI in marker *D13mit16* has.

Significantly high frequencies of MSI in markers *D13mit78* and

MARKER	CHROMOSOME LOCATION (cM)	REPEAT MOTIF	MARKER LOCATION	GENE	GENE LOCATION	GENE FUNCTION
4-4-19844	Chr19 (42.0)	(CAGGCT)30	chr19:4288135-4288414	Adrbk1	Intron 18-19	(Adrenergic receptor kinase, beta 1) cell signals involved in inflammation
D13mit16	Chr13 I (10.0)	(TG)24	chr13:20385311-20385519	Elmo1	5'Upstream 0.2Mb	(Engulfment and cell motility protein 1) protein binding, apoptosis
D13mit78	Chr13 (75.0)	(CA)25	chr13:119618032-119618260	Fgf-10	5'Upstream 0.1Mb	(Fibroblast growth factor10 precursor); cellprocesses during embryogenesis, adult tissue homeostasis, and carcinogenesis
DXmit249	ChrX(60.5)	(TG)17	chrX:160413766-160413877	Car5b	5'Upstream 0.01Mb	(Carbonic anhydrase 5b, mitochondrialgene);catalysing the interconversion of carbon dioxide and bicarbonate
D19mit68	Chr19 (6.0)	(TG)21	chr19:3645155-3645286	Lrp5	5'Upstream 0.1Mb	(Low-density lipoprotein receptor-related protein5 precursor) act as a coreceptor of Wnt-pathway

Notes: This table shows the specific chromosome location, repeat motifs, nucleotide marker location in regards to the chromosome, related genes, marker location of adjacent genes, and gene function information from NCBI, NLM, and NIH databases or from reference papers.

Table 4: Summary list of 5 informative markers and related genes.

4-4-19844 were detected in female *Sod1* knockout PGC samples, but both markers were stables in male *Sod1* knockout PGCs, as well as in male and female wild type *Sod1* and heterozygous *Sod1*+/- PGCs. Marker *D13mit78* is located near the fibroblast growth factor 10 precursor (*Fgf-10*) gene that has been linked to cell development (Tables 1.3 and 1.4). The *Fgf10* gene has been detected in normal human ovarian theca, stroma and endometrial cells that play a role in stimulating the growth of activated follicles [40]. Impairment of *Fgf10* gene expression influences paracrine signaling of cell survival, showing its importance for maintenance of follicles and follicular growth [40]. The results of this study denote that MSI on marker *D13mit78* could negatively affect early follicular development of female primordial gonads, resulting in increased risk of infertility. Marker *4-4-19844* was unstable and it is located near the adrenergic receptor kinase, beta 1(*Adrbk1* also known as *Grk2*) gene which has a key role in cell signal transduction through the process of receptor desensitization and internalization, avoiding excessive stimulation [41] (Tables 1.3 and 1.4). The follicle stimulating hormone receptor (FSHr) is a clear example of a *Grk2*transmembrane receptor which is expressed in the ovarian granulosa cells. It has been reported that Grk2 protein translation is affected by the presence of oxidative stress, giving rise to uncontrolled receptor signaling [42]. As a consequence of this, decreased expression of the *Grk2* gene has been involved in human granulosa cell tumors probably due to improper receptor desensitization and prolonged activation of FSHr [41]. Taken together, our findings suggest that high risk of female infertility and ovarian cancer could be a manifestation from MSI of markers *D13mit78* and *4-4-19844* in PGCs.

Male *Sod1* knockout PGCs were significantly unstable in one marker, *D19mit68*. MSI instability was not detected in male *Sod1* knockout PGCs or in female and male wild type *Sod1* and heterozygous *Sod1* +/- PGC samples. The marker *D19mit68* is located near low density lipoprotein receptor related protein 5 precursor (*Lrp5*) gene that acts as a cofactor of the Wnt pathway. The importance of Wnt pathway lies in many cell processes such as cell development, proliferation, fate, and death. It is known that specific mutations of genes that encode this pathway contribute to different types of cancer such as breast, ovarian, and prostate [33]. Our results suggest that MSI on marker *D19mit68* could be responsible for malignant cell transformation in male mouse PGCs in the presence of oxidative stress.

In conclusion, our results indicate that accumulation of DNA damage is present in *Sod1* knockout mice. PGC samples from *Sod1* mice at the time of migration and colonization of the gonad acquired spontaneous mutations due to oxidative stress response deficiencies by *Sod1* gene disruption. The presence of MSI during specific times in mouse embryonic development could be a signal for PGC pool selection in the female and male genital ridges and, additionally, to be the *on-switch* for cell transformation into premature ovarian failure and/or ovarian tumorigenesis when aging deterioration occurs during adult life. Extrapolation of the instability of these markers and genes in the mouse model has also been described in the human genome. Therefore, identification of target mouse genes involved during cell stress responses might shed some light toward determining mechanisms that control oxidative stress consequences in human PGCs. These novel markers might allow for useful screening methods to detect initiation, determination, and progression of premature ovarian failure or human ovarian carcinomas. Supplementary characterization of these genes and their expression status needs to be done in the future to determine the specific functions they have in the evolution of human ovarian failure or tumorigenesis.

Appendix

Isolation and derivation of mouse embryonic germinal cells (http://www. jove. com/index/Details. stp?ID=1635)

References

1. De Felici M, Dolci S, Pesce M (1992) Cellular and molecular aspects of mouse primordial germ cell migration and proliferation in culture. Int J Dev Biol 36: 205-213.

2. Pesce M, Klinger FG, De Felici M (2002) Derivation in culture of primordial germ cells from cells of the mouse epiblast: phenotypic induction and growth control by Bmp4 signalling. Mech Dev 112: 15-24.

3. Tam PP, Snow MH (1981) Proliferation and migration of primordial germ cells during compensatory growth in mouse embryos. J Embryol Exp Morphol 64: 133-147.

4. Ledda S, Bogliolo L, Bebbere D, Ariu F, Pirino S (2010) Characterization, isolation and culture of primordial germ cells in domestic animals: recent progress and insights from the ovine species. Theriogenology 74: 534-543.

5. De Felici M (2000) Regulation of primordial germ cell development in the mouse. Int J Dev Biol 44: 575-580.

6. Labosky PA, Hogan BL (1999) Mouse primordial germ cells. Isolation and in vitro culture. Methods Mol Biol 97: 201-212.

7. McLaren A (2003) Primordial germ cells in the mouse. Dev Biol 262: 1-15.

8. Resnick JL, Bixler LS, Cheng L, Donovan PJ (1992) Long-term proliferation of mouse primordial germ cells in culture. Nature 359: 550-551.

9. Essick EE, Sam F (2010) Oxidative stress and autophagy in cardiac disease, neurological disorders, aging and cancer. Oxid Med Cell Longev 3: 168-177.

10. Agarwal A, Gupta S, Sharma RK (2005) Role of oxidative stress in female reproduction. Reprod Biol Endocrinol 3: 28.

11. Carlsson LM, Jonsson J, Edlund T, Marklund SL (1995) Mice lacking extracellular superoxide dismutase are more sensitive to hyperoxia. Proc Natl Acad Sci U S A 92: 6264-6268.

12. Matzuk MM, Dionne L, Guo Q, Kumar TR, Lebovitz RM (1998) Ovarian function in superoxide dismutase 1 and 2 knockout mice. Endocrinology 139: 4008-4011.

13. Lu W, Ogasawara MA, Huang P (2007) Models of reactive oxygen species in cancer. Drug Discov Today Dis Models 4: 67-73.

14. Noor R, Mittal S, Iqbal J (2002) Superoxide dismutase--applications and relevance to human diseases. Med Sci Monit 8: RA210-215.

15. Peled-Kamar M, Lotem J, Okon E, Sachs L, Groner Y (1995) Thymic abnormalities and enhanced apoptosis of thymocytes and bone marrow cells in transgenic mice overexpressing Cu/Zn-superoxide dismutase: implications for Down syndrome. EMBO J 14: 4985-4993.

16. Ho YS, Magnenat JL, Gargano M, Cao J (1998) The nature of antioxidant defense mechanisms: a lesson from transgenic studies. Environ Health Perspect 106 Suppl 5: 1219-1228.

17. Watanabe K, Shibuya S, Ozawa Y, Nojiri H, Izuo N, et al. (2014) Superoxide dismutase 1 loss disturbs intracellular redox signaling, resulting in global age-related pathological changes. Biomed Res Int 2014: 140165.

18. Noda Y, Ota K, Shirasawa T, Shimizu T (2012) Copper/zinc superoxide dismutase insufficiency impairs progesterone secretion and fertility in female mice. Biol Reprod 86: 1-8.

19. Ho YS, Gargano M, Cao J, Bronson RT, Heimler I, et al. (1998) Reduced fertility in female mice lacking copper-zinc superoxide dismutase. J Biol Chem 273: 7765-7769.

20. Moreno-Ortiz H, Esteban-Perez C, Badran W, Kent-First M (2009) Isolation and derivation of mouse embryonic germinal cells. J Vis Exp .

21. Nagamine CM, Chan KM, Kozak CA, Lau YF (1989) Chromosome mapping and expression of a putative testis-determining gene in mouse. Science 243: 80-83.

22. Coolbaugh-Murphy M, Maleki A, Ramagli L, Frazier M, Lichtiger B, et al. (2004) Estimating mutant microsatellite allele frequencies in somatic cells by small-pool PCR. Genomics 84: 419-430.

23. Coolbaugh-Murphy MI, Xu J, Ramagli LS, Brown BW, Siciliano MJ (2005) Microsatellite instability (MSI) increases with age in normal somatic cells. Mech Ageing Dev 126: 1051-1059.

24. Zhang Y, Monckton DG, Siciliano MJ, Connor TH, Meistrich ML (2002) Detection of radiation and cyclophosphamide-induced mutations in individual mouse sperm at a human expanded trinucleotide repeat locus transgene. Mutat Res 516:121-138.

25. Coolbaugh-Murphy MI, Xu JP, Ramagli LS, Ramagli BC, Brown BW, et al. (2010) Microsatellite instability in the peripheral blood leukocytes of HNPCC patients. Hum Mutat 31: 317-324.

26. Elchuri S, Oberley TD, Qi W, Eisenstein RS, Jackson Roberts L, et al. (2005) CuZnSOD deficiency leads to persistent and widespread oxidative damage and hepatocarcinogenesis later in life. Oncogene 24: 367-380.

27. Bendel-Stenzel M, Anderson R, Heasman J, Wylie C (1998) The origin and migration of primordial germ cells in the mouse. Semin Cell Dev Biol 9: 393-400.

28. Matsui Y (1998) Developmental fates of the mouse germ cell line. Int J Dev Biol 42: 1037-1042.

29. Miana-Mena FJ, González-Mingot C, Larrodé P, Muñoz MJ, Oliván S, et al. (2011) Monitoring systemic oxidative stress in an animal model of amyotrophic lateral sclerosis. J Neurol 258: 762-769.

30. Van Remmen H, Qi W, Sabia M, Freeman G, Estlack L, et al. (2004) Multiple deficiencies in antioxidant enzymes in mice result in a compound increase in sensitivity to oxidative stress. Free Radic Biol Med 36: 1625-1634.

31. Huang TT, Yasunami M, Carlson EJ, Gillespie AM, Reaume AG, et al. (1997) Superoxide-mediated cytotoxicity in superoxide dismutase-deficient fetal fibroblasts. Arch Biochem Biophys 344: 424-432.

32. Gatcliffe TA, Monk BJ, Planutis K, Holcombe RF (2008) Wnt signaling in ovarian tumorigenesis. Int J Gynecol Cancer 18: 954-962.

33. Johnson ML, Rajamannan N (2006) Diseases of Wnt signaling. Rev Endocr Metab Disord 7: 41-49.

34. Busuttil RA, Garcia AM, Cabrera C, Rodriguez A, Suh Y, et al. (2005) Organ-specific increase in mutation accumulation and apoptosis rate in CuZn-superoxide dismutase-deficient mice. Cancer Res 65: 11271-11275.

35. Philips T, Robberecht W (2011) Neuroinflammation in amyotrophic lateral sclerosis: role of glial activation in motor neuron disease. Lancet Neurol 10: 253-263.

36. Woelber L, Mueller V, Eulenburg C, Schwarz J, Carney W, et al. (2010) Serum carbonic anhydrase IX during first-line therapy of ovarian cancer. Gynecol Oncol 117: 183-188.

37. Hynninen P, Vaskivuo L, Saarnio J, Haapasalo H, Kivelä J, et al. (2006) Expression of transmembrane carbonic anhydrases IX and XII in ovarian tumours. Histopathology 49: 594-602.

38. Wang H, Linghu H, Wang J, Che YL, Xiang TX, et al. (2010) The role of Crk/Dock180/Rac1 pathway in the malignant behavior of human ovarian cancer cell SKOV3. Tumour Biol 31: 59-67.

39. Jarzynka MJ, Hu B, Hui KM, Bar-Joseph I, Gu W, et al. (2007) ELMO1 and Dock180, a bipartite Rac1 guanine nucleotide exchange factor, promote human glioma cell invasion. Cancer Res 67: 7203-7211.

40. Chaves RN, Lima-Verde IB, Celestino JJ, Duarte AB, Alves AM, et al. (2010) Fibroblast growth factor-10 maintains the survival and promotes the growth of cultured goat preantral follicles. Domest Anim Endocrinol 39: 249-258.

41. King DW, Steinmetz R, Wagoner HA, Hannon TS, Chen LY, et al. (2003) Differential expression of GRK isoforms in nonmalignant and malignant human granulosa cells. Endocrine 22: 135-142.

42. Cobelens PM, Kavelaars A, Heijnen CJ, Ribas C, Mayor F Jr, et al. (2007) Hydrogen peroxide impairs GRK2 translation via a calpain-dependent and cdk1-mediated pathway. Cell Signal 19: 269-277.